Ground Robot-based Sensing Device with Launcher-Retrieval System for Volcano Crater Lake pH and Temperature Monitoring

Kate Ira Augusto, Jeanette Pao, *Member, IAENG,* Immanuel Paradela, Charles Alver Banglos, and Carl John Salaan, *Member, IAENG*

***Abstract*—Changes in volcanic activity are frequently correlated with geochemical changes in crater lake waters. Volcanologists employ periodic surveys of the volcano crater lake which include pH and temperature monitoring. Due to the exposure of volcanologists to volcanic hazards, a robotic remote monitoring system was implemented in this study.**

A ground robot with a tethered sensing device, launcher, and retrieval system is investigated for pH and temperature real-time data sensing considering the challenging conditions of Taal Crater Lake in the Philippines. The sensing device has a tethering system attached to two mechanisms: the launcher and the retrieval systems. From the test experiments, it was found that the system can project the sensing device for a horizontal distance of 3 meters and retrieve it smoothly.

The pH and temperature sensors in the device were calibrated and demonstrated acceptable levels of error and reliability. An actual test on a lake environment was implemented. The remote-controlled ground robot can navigate the sensing device to the required default position near the lake shore and effectively launch the sensing device into the water. Moreover, the tethered sensing device successfully performed real-time pH and temperature data sensing of the water and was securely retrieved from the water back to the ground robot. After the real-time data were assessed and validated, the average errors for the temperature and pH data were only 0.44% and 1.8%, respectively.

***Index Terms*—ground robot, tethered sensing device, Taal volcano, pneumatic launcher, temperature sensing, pH data sensing, real-time data sensing.**

I. Introduction

Taal Volcano, the second most active volcano in the Philippines, is located in Batangas, Luzon. It is a stratovolcano situated in the center of Taal Lake and is the most lethal of the 24 active volcanoes in the country [1].

Manuscript received November 30, 2023; revised April 4, 2024.

This research was funded by the Department of Science and Technology—Engineering Research and Development for Technology (DOST-ERDT) and supported by the Philippine Council for Industry, Energy, and Emerging Technology Research and Development (DOST-PCIEERD) and the Philippine Institute of Volcanology and Seismology (PHIVOLCS).

K. I. Augusto is a graduate student at the Center for Mechatronics and Robotics, Mindanao State University – Iligan Institute of Technology, Iligan City, Philippines (e-mail: kateira.augusto@g.msuiit.edu.ph).

J. Pao is a researcher at the Center for Mechatronics and Robotics, Mindanao State University – Iligan Institute of Technology, Iligan City, Philippines (e-mail: jeanette.pao@g.msuiit.edu.ph).

I. Paradela is a researcher at the Center for Mechatronics and Robotics, Mindanao State University – Iligan Institute of Technology, Iligan City, Philippines (e-mail: immanuel.paradela@g.msuiit.edu.ph).

C. A. Banglos is a researcher at the Center for Mechatronics and Robotics, Mindanao State University – Iligan Institute of Technology, Iligan City, Philippines (e-mail: charlesalver.banglos@g.msuiit.edu.ph).

C. J. Salaan is a professor at the Center for Mechatronics and Robotics, Mindanao State University – Iligan Institute of Technology, Iligan City, Philippines (e-mail: carljohn.salaan@g.msuiit.edu.ph).

Fig. 1. The ground robot with a sensing device and launching and retrieval mechanisms designed for crater lake geochemical monitoring.

The Philippine Institute of Volcanology and Seismology (PHIVOLCS) implies that changes in volcanic activity are often correlated with geochemical changes in crater lake waters and hot springs, making them valuable monitoring parameters [2]. That is why Philippine volcanologists conduct periodic surveys of Taal Volcano Lake, including pH and temperature data sensing. However, traditional on-site monitoring exposes volcanologists to hazardous volcanic chemicals and eruption danger. Through volcano monitoring, volcanologists can assess the volcano's condition and identify changes that could pose volcanic threats [3], [4], [5].

The main crater lake, an acidic lake with a pH of 3, stands out as the most notable feature of Taal Volcano's extensive hydrothermal system. Situated at the core of an active vent complex, it is surrounded by Lake Taal, a slightly alkaline caldera lake. Taal is prone to regular hydrovolcanic eruptions, which can occasionally be catastrophic owing to its unusual location. In 1991, 1992, and 1995, researchers collected samples of fumaroles, hot springs, and lake waters to develop a geochemical model of the hydrothermal system [6]. The study by [7] involves strategically collecting water samples from Taal Volcano's crater lake, offering insights into the interplay between volcanic activity and geochemical changes. Previous studies on the water chemistry of Taal Crater Lake have provided valuable insights into its chemical composition, revealing changes and heightened CO_2 emissions correlated with seismic unrest during volcano-seismic disturbances [8].

Several studies have utilized Unmanned Ground Vehicles (UGVs) or ground robots for volcano applications, aiding in the exploration of volcanoes [9], [10], [11], [12], [13], [14]. Another effective method for obtaining vital information

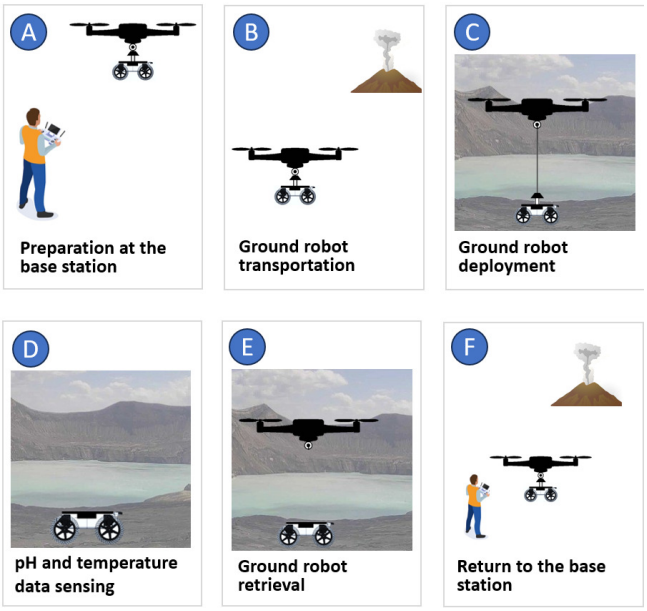

Fig. 2. The general procedure for deploying the ground robot with a sensing device near the volcano crater involves several steps from preparation at the base station, transportation of the device, release to the ground, data-gathering mission, and return to the base station.

Fig. 3. An example of actual deployment operation of the ground robot utilizing a high payload drone. The drone carrying the ground robot will transport the ground robot to the area of deployment.

in volcanic zones is the use of Unmanned Aerial Vehicles (UAVs) [15], [16], [17]. UAVs typically have a limited flight duration, making ground robots well-suited for extended exploration periods. However, ground robots may face constraints in accessing regions obstructed by rugged terrain. Therefore, a synergistic approach where ground robots deploy and retrieve ground robots to and from volcanic areas presents an ideal solution [18]. Despite the advantages of a robotic remote observation system in minimizing risks to volcanologists and technicians during eruptive phenomena, current ground robots still face difficulties in performing crater lake monitoring beyond their immediate vicinity. However, through the innovative use of a pneumatic launcher integrated into a mobile robot, the robot can extend its monitoring capabilities.

As shown in Fig. 1, the ground robot used has wheels that can effectively traverse the terrains near the lake, and the de-

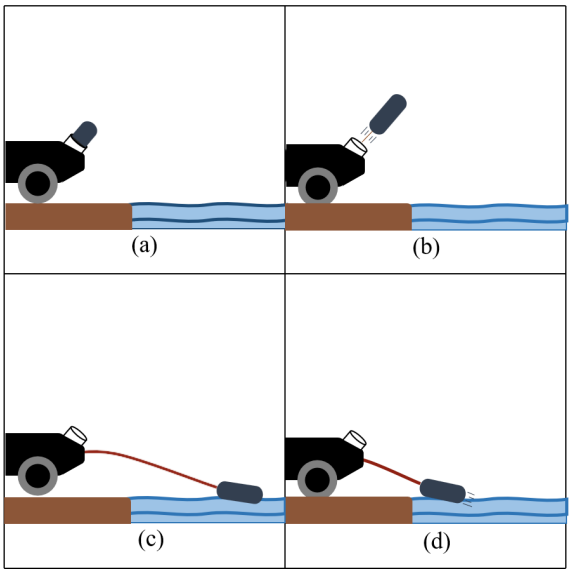

Fig. 4. The general procedure for deploying the sensing device to the volcano crater lake and data gathering operation. The sensing device is initially at default position near the crater lake (a). The sensing device is then launched into the crater lake (b) and starts gathering pH and temperature data of the lake (c). Lastly, the sensing device is retrieved back to the ground robot (d).

veloped sensing device with a launching and retrieval system was investigated in this study, focusing on the performance of the system for real-time pH and temperature data sensing.

The general concept for volcano crater lake data sensing utilizing a sensing device with a launcher and retrieval mechanism is illustrated in Fig. 2, Fig. 2, and Fig. 4. Considering the design requirements based on Taal Volcano conditions, this concept will enable the deployment of the sensing device into the crater lake, facilitating real-time data measurements and retrieving the device after a substantial period.

II. Design Considerations and Methodologies

This chapter introduces the design considerations and methodologies employed to fulfill this study's objectives. As illustrated in Fig. 5, the study began by identifying the requirements and specifications for developing a ground robot-based crater lake monitoring system. This was accomplished by conducting comprehensive information gathering to evaluate the condition of the crater lake, determine the parameters in need of monitoring, and devise suitable data acquisition methods. Additionally, an optimal robot platform was identified. Once the necessary information was gathered, the design phase commenced. Detailed analysis was conducted to develop a sensing device, launcher, and retrieval mechanism for deploying and retrieving the device from the crater lake area. After the design and analysis phase, the fabrication methods were planned and executed. Each device and mechanism was developed and subjected to individual testing and evaluation to ensure their effectiveness. Upon obtaining satisfactory results, they were integrated into the ground robot. The entire system underwent testing and evaluation during field tests.

The system operates by deploying a specially designed sensing device into Taal Crater Lake. This sensing device is equipped with sensors capable of measuring and recording important lake parameters, specifically pH and temperature.

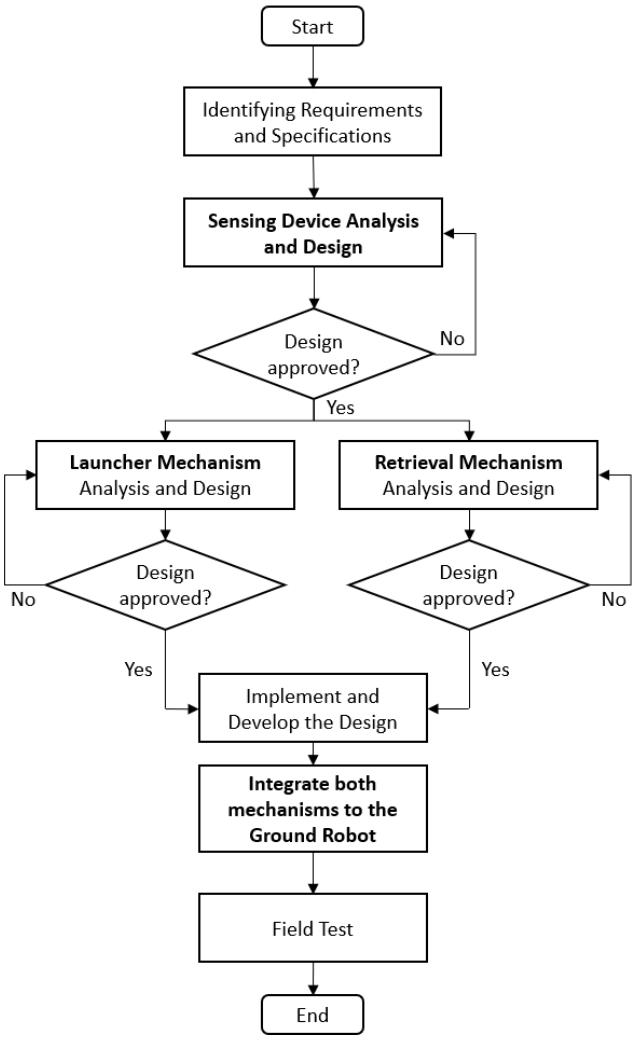

Fig. 5. The process flow in developing the pH and temperature sensing device with its launching and retrieval mechanisms installed on the ground robot.

Once the sensing device is deployed into Taal Crater Lake, it begins collecting real-time data from the sensors. The monitoring system continues to gather data from the sensors for a substantial period, ensuring a comprehensive dataset is acquired.

A. Data Gathering of Taal Volcano Crater Condition

Monitoring the chemistry and temperature of groundwater, surface water, and steam at a volcano can provide valuable insights into changes in volcanic activity over time. Through evaluation and direct communication with the Philippine Institute of Volcanology and Seismology (PHIVOLCS), it was gathered that the temperature of the crater lake typically ranges between 65°C and 80°C when the alert level is categorized within the range of 2 to 3. However, in this study, ground robot deployment, exploration, and monitoring will only be conducted during normal operation of volcano monitoring (no warning level).

B. Evaluation of Possible Launching Areas

Actual images and data of Taal Volcano Crater Lake were provided by PHILVOLCS. In Fig. 6, the shoreline of the volcano crater and potential deployment areas for the ground

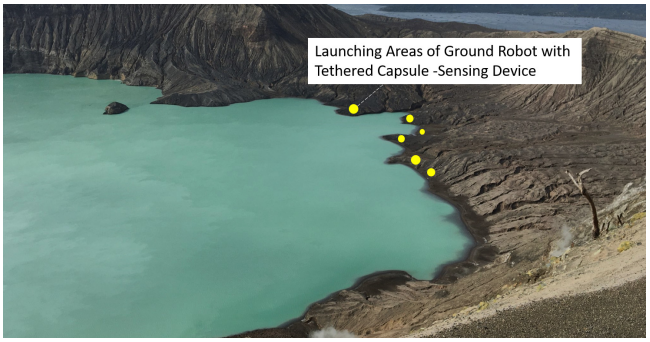

Fig. 6. The launching areas found near the Taal crater lake shore where the ground robot can deploy the sensing device on the lake water.

robot, where it will launch the tethered sensing device into the crater water, can be observed. These deployment areas are flat, with a slight incline that allows the ground robot to position itself 0.5 to 1 meter away from the water.

C. Launching Distance Design Consideration

Additionally, crater lake sampling is conducted 3 to 5 meters from the shoreline of the lake. Following consultations and in-person evaluations with PHIVOLCS, this study implemented a compact launcher mechanism capable of projecting the sensing device a minimum distance of 3 meters from the ground robot's default position. Furthermore, a retrieval mechanism designed to recover the sensing device once a substantial amount of data has been accumulated was integrated.

D. Ground Robot Platform Selection

The ground robot utilized in this study shares similarities with the mobile robot presented in previous research [14]. The design requirements for the ground robot were determined based on the environmental conditions, as discussed in previous sections. Specifically, the ground robot's wheels were designed to navigate uneven terrain and surmount obstacles like rocks. Careful consideration was given to appropriately sizing the wheels to facilitate effective obstacle climbing. The wheels were engineered to withstand pressure from pointy rocks by allowing deformation and restoring their original shape to enhance durability. Furthermore, the chosen body frame material provided ample safeguarding for the electronic components, ensuring their proper operation within the specified temperature limits.

E. Sensing Device Overall Design Requirements

After identifying the necessary conditions, the design requirements for the crater Lake monitoring system were established. These requirements are specifically tailored for the selected ground robot platform. The monitoring system is designed to meet the following specifications:

1) A sensing device capable of real-time monitoring of pH and temperature levels.
2) A compact launcher mechanism with the ability to project the sensing device a minimum distance of 3 meters away from the ground robot.
3) A retrieval mechanism designed to recover the sensing device once a substantial amount of data has been accumulated.

F. Testing and Evaluation Methods

The sensors and control units will undergo evaluation tests to assess the performance of the monitoring system. These tests will focus on three key characteristics: sensitivity, accuracy, and reliability. Sensitivity refers to the sensors' ability to detect and convey changes in readings quickly. This aspect will be evaluated to ensure that the sensors can promptly capture any variations in the monitored parameters. Accuracy refers to the sensors' ability to provide correct measurements, while reliability pertains to their ability to deliver consistent and dependable readings. These aspects are crucial for ensuring reliable data capture. Additionally, the control units will be tested for their responsiveness to user commands, their ability to function according to the assigned tasks, and the consistency of their results. Overall, these evaluation tests will help assess the performance of the sensors and control units, ensuring the monitoring system's effectiveness and reliability.

1) Distance Test: A launch distance test is conducted to verify if the capsule can be launched at a minimum distance of 3 meters. Prior to the launch, the area around the air valve is carefully inspected to ensure there is no air leakage.

2) Retrieval Test: A retrieval test is performed to ensure the safe and successful retraction of the capsule-shaped sensing device back into the ground robot after completing its assigned task.

3) Sensor Test: To evaluate the performance of the pH and temperature sensors, their data is compared to readings obtained from reliable instruments, namely a portable pH meter for the pH sensor and a laboratory thermometer for the temperature sensor. The percentage difference between the sensor data and the reference instruments is calculated.

4) Actual Test: Following the completion of the aforementioned tests, an actual field test is conducted to validate the system's functionality in a simulated environment. Due to limitations in time and resources, the field test is carried out near a river, chosen for its similarities to an actual volcano crater lake environment. This field test serves as a final assessment to ensure the system's functionality.

III. Sensing Device Propose Design and Mechanisms

A. Proposed Components for the Sensing Device

As mentioned in the previous section, monitoring the chemistry and temperature of groundwater, surface water, and steam at a volcano can provide valuable insights into changes in volcanic activity over time. In this study, the sensing device used to monitor the lake water is in the form of a capsule, offering advantages such as compactness, equipment protection, and easy deployment and retrieval. The capsule is protected by a waterproof and high-strength epoxy coating, which is specifically designed to withstand the extreme temperatures experienced in the lake environment. This epoxy coating provides both heat resistance and high psi strength, ensuring the durability and integrity of the capsule even under harsh conditions.

To ensure independent operation, the capsule is equipped with its own power system, consisting of a lightweight 3.7V battery and an Arduino Nano microcontroller unit (MCU). The capsule contains two sensors, a pH sensor and a temperature sensor, as recommended by PHIVOLCS. Real-time data from these sensors can be wirelessly transmitted. Fig. 7 depicts the schematic diagram of the proposed sensing device.

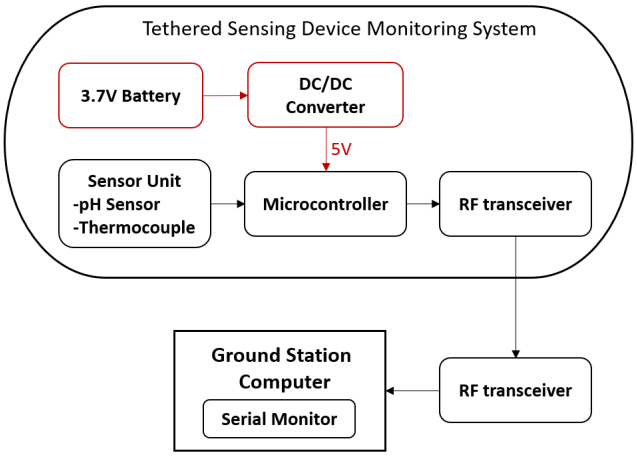

Fig. 7. The schematic diagram of the pH and temperature sensing device.

For efficient retrieval, the capsule is attached to a multifilament fishing line, selected for its exceptional tensile strength and resistance to abrasion. This type of fishing line provides reliability and durability during the retrieval process.

B. The Launcher Mechanism and its Main Components

The primary objective of the launch system is to propel the tethered probe towards the crater lake, ensuring it achieves a minimum distance of 3 meters from the robot. To accomplish this, the launch mechanism is specifically designed to provide sufficient acceleration.

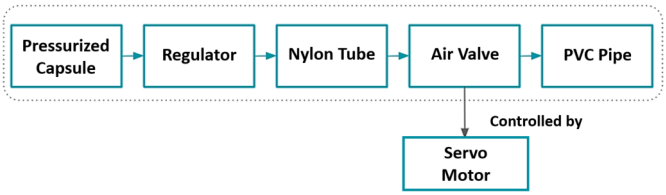

Fig. 8. The main components of the launcher mechanism of the sensing device.

The components of the system need to be compact in size to fit within the robot's constraints. The key components of the developed system include Pressurized Air, which serves as the propeller, an air pressure regulator to control the released air pressure, a nylon tube that connects the regulator to an air valve, and a servo motor responsible for switching the valve on and off. Fig. 8 provides a block diagram of the components needed for the launcher mechanism.

C. The Retrieval Mechanism and its Main Components

The retrieval mechanism plays a critical role in the safe recovery of the sensing device after collecting a sufficient amount of data. In this study, a specialized reeling mechanism was developed for this purpose.

The mechanism consists of several essential components, including a switch relay and motor driver, which effectively

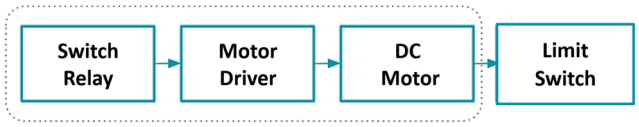

Fig. 9. The main components of the retrieval mechanism of the sensing device.

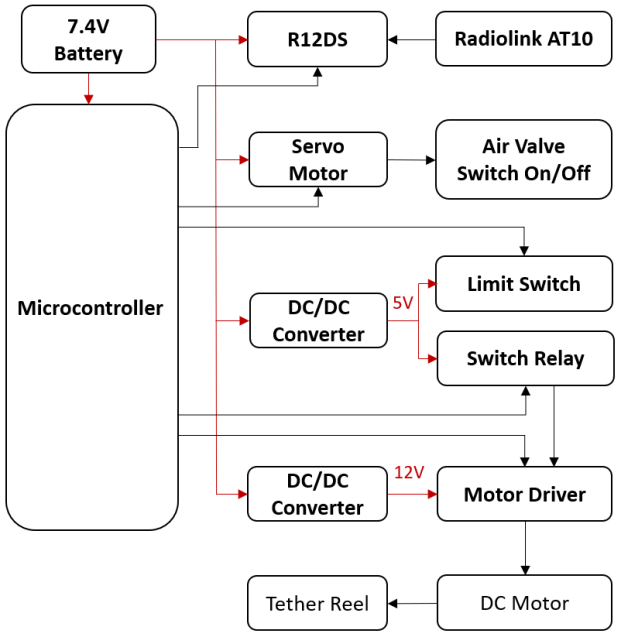

Fig. 10. The schematic diagram of the launcher and retrieval system for the sensing device.

control the DC motor responsible for winding the multifilament line connected to the sensing device. Additionally, a limit switch is integrated into the system, which is triggered by the capsule sensing device once it is inside the robot, signaling the DC motor to stop reeling. To control these actuators, a wireless communication system is utilized. The block diagram of the components for the retrieval mechanism is shown in Fig. 9.

D. The Overall Schematic Diagram of Launcher and Retrieval System

The schematic diagram in Fig. 10 illustrates the connections and interactions between components of the launcher and retrieval mechanism. Notably, the two mechanisms share important resources such as a microcontroller, power source, and R12DS channel. DC converters are included to supply the necessary voltage for components that require different voltages from the main power source of 7.4V. The microcontroller acts as the central control unit, coordinating the operations of both mechanisms. It receives instructions and commands through the R12DS channel, serving as the communication interface between the system and the operator. This allows remote control and monitoring of the launching and retrieval processes. To ensure compatibility with various voltage requirements, DC converters are integrated into the system. These converters adapt the input voltage to match the specific needs of individual components. By using these converters, components that operate on different voltages than

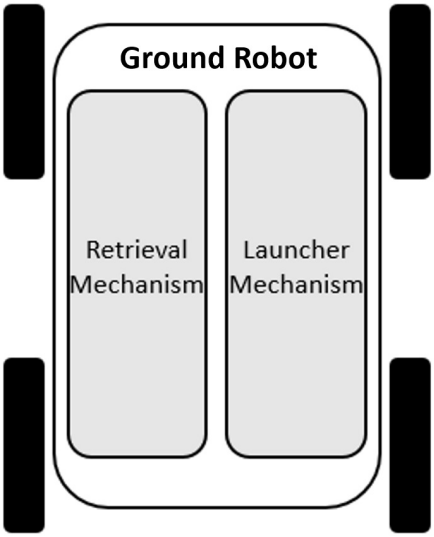

Fig. 11. The integration of launcher and retrieval mechanisms into the ground robot platform.

the main power source (7.4V) can be seamlessly incorporated into the system.

Fig. 11 illustrates the integration of the two mechanisms on the ground robot platform used in this study. In this setup, the launcher and retrieval system components can be positioned properly inside the ground robot body.

IV. Theoretical Analysis

A. Launching System

Theoretical considerations for the launching system were analyzed in this section to design the permissible overall weight of the sensing device and achieve its 3-meter range of motion. The design parameters are illustrated in Fig. 12.

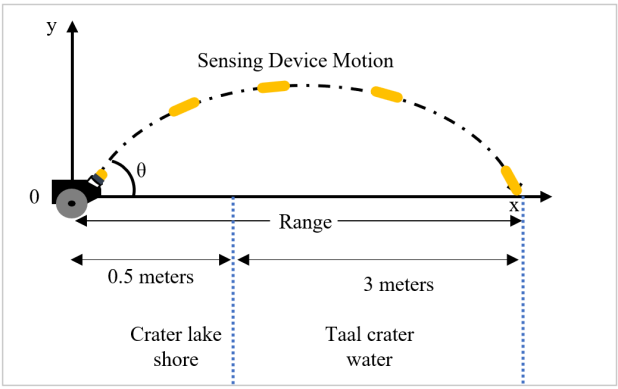

Fig. 12. The parameters for the sensing device's required launching velocity to achieve a distance of 3 meters.

The motion of an object hurled into the air is known as projectile motion. The horizontal distance traveled by the projectile, *Range*, can be calculated using the formula:

$$Range = \frac{v^2\,(sin(2\theta))}{g} \tag{1}$$

$$v = \sqrt{\frac{Range\,(g)}{sin(2\theta)}} \tag{2}$$

where v is the initial velocity of the projectile, θ is the launch angle, and g is the acceleration due to gravity.

The initial velocity of the projectile can be calculated using Equation 2. Given that the launch angle is 45 degrees and the required horizontal distance traveled (range) is 3 meters, the velocity needed to achieve this distance for the given projectile and launch angle is approximately 5.42 m/s.

The required velocity for the sensing device can be attained by applying force to the capsule body (sensing device). Thus, pressure over the area of application on the capsule base was calculated to determine the integrated pressurizer device for the launcher. Applying the conservation of energy, which states that energy cannot be created or destroyed but only transformed from one form to another:

$$\frac{1}{2}mv^2 = nRT - PV_{initial} \tag{3}$$

In this study, a CO_2 cartridge, which is a highly compressed cylinder of liquid carbon dioxide was integrated. As the liquid CO_2 is released, it rapidly turns into a gas, facilitating the quick release of the compressed CO_2 and enabling the propulsion or launch of the sensing device capsule.

The pressure needed to convert the potential energy of the compressed CO_2 into the kinetic energy of the projectile, where n is the number of moles, R is the ideal gas constant, V initial is the initial volume of compressed CO_2, m is the mass of the projectile, and v is its velocity, can be calculated by rearranging this equation to:

$$P = \frac{nRT - \frac{1}{2}mv^2}{V_{initial}} \tag{4}$$

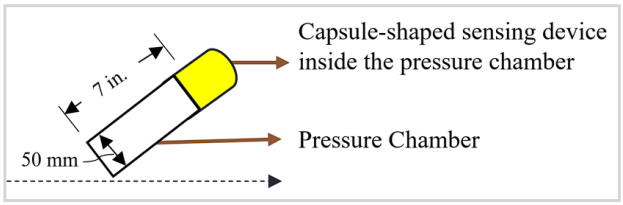

Fig. 13. The determination of the weight of the sensing device and the dimensions of the pressure chamber are necessary to calculate the required pressure for launching the sensing device.

Given that the projectile mass is 186 grams, the terminal velocity of 5.42 m/s and the diameter of the pressure chamber was set to 50 mm, having a length of 7 inches where the capsule-shaped sensing device was inserted, shown in Fig. 13. Considering the launching of the sensing device capsule through the CO_2 cartridge, the mass of CO_2 gas utilized is 12 grams at a room temperature of 298 K. The number of moles of CO_2 will be used to calculate the volume of the pressure chamber and its corresponding pressure value. The calculated number of moles of CO_2 is equal to 0.2727 moles.

$$n_{CO2} = \frac{m_{CO2}}{molar\ mass\ of\ CO_2} \tag{5}$$

The calculated volume of the pressure chamber, V, and substituting the known values into the pressure using equation 4, through the following:

$$A = \pi(\frac{d}{2}^2) \tag{6}$$

$$V = A(L) \tag{7}$$

Thus, it was found that the volume of the pressure chamber, V, is about 0.0001735 m^3, and the approximate value of pressure needed is approximately 0.992 MPa. This calculation considered the idealized scenario and neglected factors such as air leakage, friction, and other non-ideal conditions that may affect the actual pressure required in practice.

B. Servo Motor Torque Consideration

To determine the required torque to open the valve, equation 8 is utilized:

$$\tau = F(l) \tag{8}$$

where τ is the torque required, F is the applied force, and l is the moment arm, as shown in Fig. 14 First, the force acting on the valve due to the pressure difference is calculated. The force can be determined using the formula of force in equation 9 below. The area of the valve can be calculated using the formula for the area of a circle of radius r in equation 10.

$$F = P_{applied}(Area) \tag{9}$$

$$Area = \pi(r^2) \tag{10}$$

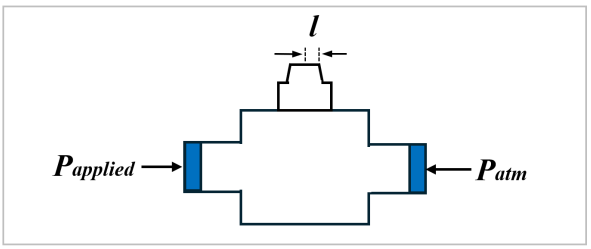

Fig. 14. The launcher parameters for considering servo motor torque, where $P_{applied}$ represents the applied pressure and P_{atm} represents the atmospheric pressure.

And given that the diameter of the valve available is 6 mm, the radius is half of that, which is 3 mm or 0.003 m. Therefore, the area of the valve is 0.00002827 m^2. Next, the force acting on the valve due to the pressure difference, as shown in Fig 14, is equal to 135.3 psi or 0.932785 MPa. Thus, the force applied is 26.375 N. Finally, the torque required to open the valve using equation 8 is 0.210 N-m (Netwon-meter).

Considering the safety factor of 2.5 [19], the selected servo motor has a rating of 3.4335 N-m. Since the motor's torque is greater than the required torque, the motor is able to open the valve.

V. PH AND TEMPERATURE SENSOR CALIBRATION AND EVALUATION

The pH and temperature sensors undergo a calibration procedure before being evaluated. Their readings are compared with data obtained from a reliable instrument, the pH meter, to ensure accuracy. The percentage difference between

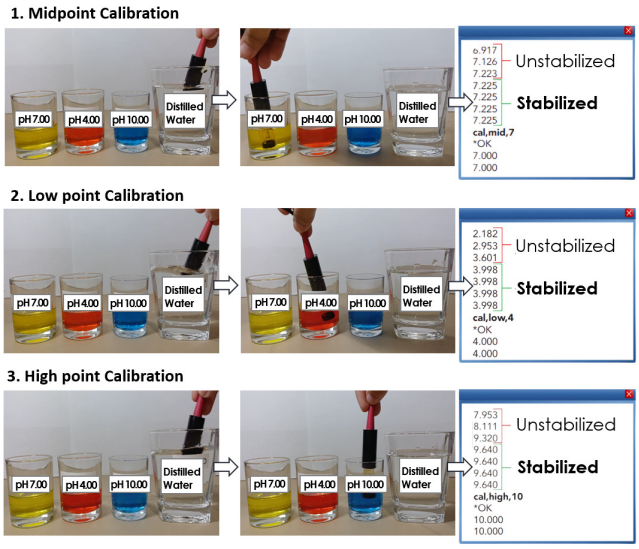

Fig. 15. The pH Sensor calibration set-up using a 3-point calibration method: midpoint calibration, low point calibration, and high point calibration.

Fig. 16. The data gathering procedure using pH meter (a) and pH sensor (b) for three liquids: liquid A (matcha latte), liquid B (tap water), and liquid C (bleach).

the sensor data and the reference instrument readings is then calculated, providing an assessment of the sensors' performance.

A. pH Sensor Testing Set-up and Calibration

Any measurement taken by the pH sensor will be wirelessly transmitted and received instantaneously using transceivers. The data will be displayed on the computer's serial monitor. First, the pH sensor and pH meter undergo calibration using a 3-point calibration method. The calibration process follows a specific order: starting with the middle pH, followed by the low pH (acidic) and high pH (basic) buffer solutions.

Fig. 15 illustrates the pH meter test setup for calibration, which involves four glasses, each containing different pH buffer solutions. The first glass contains a solution with a pH level of 6.86. Simultaneously, the second and third glasses contain solutions with pH levels of 4.00 and 9.18, respectively. Additionally, the fourth glass at the back contains distilled water used to rinse the sensor probes after they have been submerged in a solution.

To begin the calibration process, the pH meter's electrode is immersed in the 6.86 pH buffer solution. The calibrate button is pressed, and the meter is allowed to stabilize. The electrode is then removed from the buffer solution and rinsed with distilled water. This process is repeated for the 4.00 pH and 9.18 pH buffer solutions. For the calibration of the pH

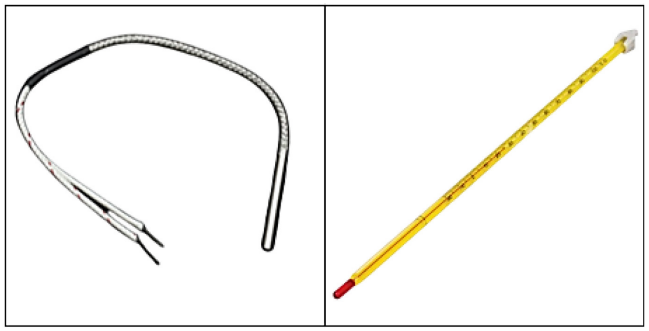

Fig. 17. The thermocouple, K-Type Thermocouple, (a) and the laboratory Thermometer (b) used in the test.

sensor, the pH probe is rinsed in water and air-dried. It is then dipped into the pH 7.00 buffer solution, stirring until the pH readings stay consistent. The pH reading and the known pH of the buffer solution are recorded. This process is repeated for the pH 4.00 and pH 10.00 buffer solutions, as shown in Fig. 15.

Once the calibration of both pH sensing devices is complete, they are tested on three liquids: liquid A (matcha latte), liquid B (tap water), and liquid C (bleach), shown in Fig. 16. Each sensor measures the pH of each solution alternatively for a total of 10 times.

B. Temperature Sensor Testing Set-up and Calibration

The measurements obtained from the thermocouple are transmitted using transceivers. In the test setup, both the thermocouple and laboratory thermometer are submerged simultaneously in the same glass of water. Fig. 17 illustrates the thermocouple and laboratory thermometer utilized in the test. To calibrate the thermocouple, its readings are compared to the values obtained from a laboratory thermometer known for its proven accuracy and reliability. This comparison allows for the alignment of the thermocouple readings with the established standards of precision and dependability set by the laboratory thermometer.

VI. Launcher and Retrieval System Design

A. Launcher System Design

The system's launching and retrieval mechanism is responsible for deploying and recovering the sensing device in Taal Crater Lake. Since existing small-scale technology for tether deployment and retrieval is limited, a novel mechanism has been devised and presented considering the Taal Crater Lake's possible launching areas. Both systems operate wirelessly through RadioLink, providing seamless control and communication.

To achieve a minimum distance of 3 meters from the robot, the launching mechanism propels the tethered probe with sufficient acceleration while being compact enough to fit within the robot's constraints. The components include Pressurized Air as the propeller, an air pressure regulator, a nylon tube, and a servo motor for valve control. It is crucial to select an air valve and nylon tube that can withstand the required pressure for launching the sensing device effectively. For safe recovery after data collection, a specialized reeling

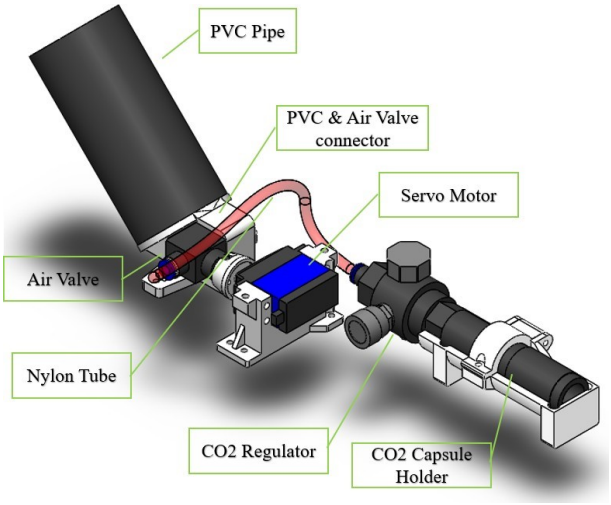

Fig. 18. The components for the launcher system, which operates wirelessly through RadioLink for seamless control and communication.

mechanism with a switch relay, motor driver, and limit switch is developed.

The CO_2 capsule is capable of releasing air pressure typically at a range of 5.5 MPa when operating at a temperature of 304 K. The CO_2 regulator is designed to regulate pressure within the range of 0-10.3 MPa. The nylon tube is specifically designed for operation at a pressure of 2.06 MPa and can withstand up to 6 MPa of air pressure.

To initiate the launching process, the capsule is initially positioned at a 45-degree angle. A PVC pipe is utilized as the capsule's container tube, illustrated in Fig. 18. A servo motor controls the activation and deactivation of the air valve. By switching the valve on, compressed air is released from the regulator, propelling the capsule-sensing device out of the tube.

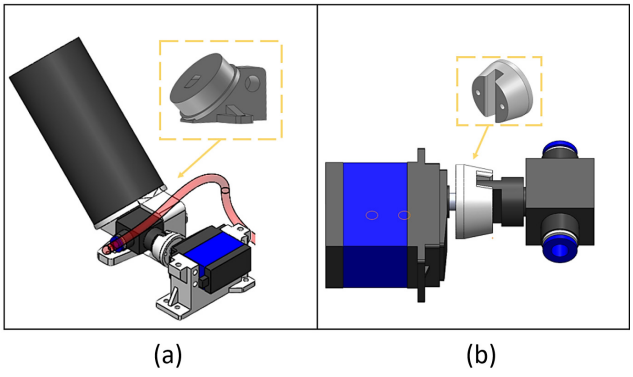

Fig. 19. The designed connector to facilitate the proper integration of the servo motor and air valve in the system (a) and another connector to ensure a secure connection between the air valve and PVC pipe (b)

A connector was designed to facilitate the proper integration of the servo motor and air valve in the system, shown in Fig. 19 (a). Similarly, a connector was created to ensure a secure connection between the air valve and PVC pipe, depicted in Fig. 19 (b). All connectors and needed supports of the overall assembly were designed using computer-aided design software and fabricated using a 3D printer.

B. Retrieval System Design

For the retrieval process, a DC motor winds the monofilament line connected to the capsule. To control the motor's operation, a switching relay regulates the power supply to the motor. The motor driver controls the rotation direction of the motor. Also, a limiting switch is strategically positioned to detect when the probe is inside the robot, triggering the DC motor to stop reeling.

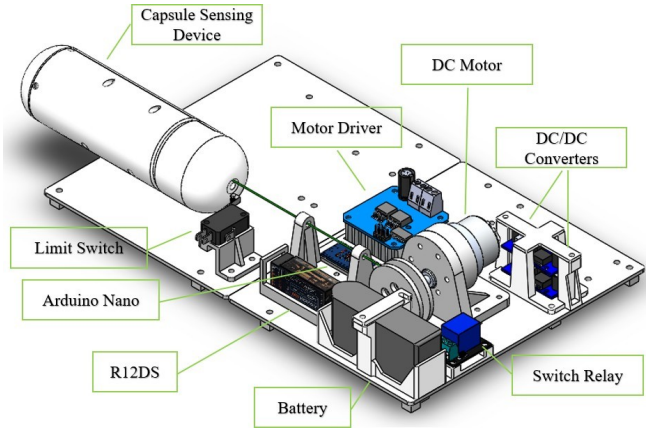

Fig. 20. The components for the retrieval system with supporting mechanism designed to guide the capsule's entry into the robot.

Fig. 20 illustrates the retrieval mechanism that ensures the safe recovery of the capsule-shaped sensing device where the ph and temperature sensors are housed once substantial data is obtained.

C. Launching and Retrieval System Integration

The launching and retrieval system is integrated into a ground robot, as depicted in Fig. 21, showcasing how the system is housed within the ground robot's body. The ground robot used is designed for volcano exploration and aligns with the studies of [14] and [20]. The pH and temperature sensors are housed inside the capsule-shaped sensing component. The overall components of the launching and retrieval system are positioned properly considering the sensing device's assembly.

D. Launching Distance Initial Testing and Evaluation

The sensors and control units undergo evaluation tests for sensitivity, accuracy, and reliability. A launch distance test verifies a minimum 3-meter launch, ensuring no air leakage. A retrieval test ensures the capsule's successful retraction. To evaluate the performance of the pH and temperature sensors, their data is compared to readings obtained from reliable instruments, namely a portable pH meter for the pH sensor and a laboratory thermometer for the temperature sensor. The percentage difference between the sensor data and the reference instruments is calculated.

VII. Results and Discussion

A. Developed pH and Temperature Data Sensing Device

In this study, the compact capsule-shaped sensing device houses all necessary components for fixed positioning from launching to retrieval, allowing easy installation of sensors

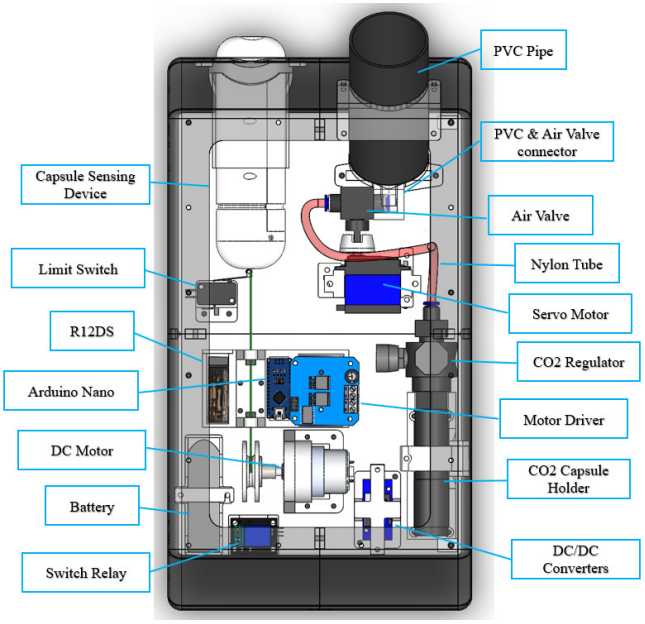

Fig. 21. The 3D model of the launcher and retrieval system components inside the ground robot body.

and other internal components. The capsule shape is designed using Computer-aided modeling software and fabricated its shape using a 3D printer. The quality of the material is ABS plastic, which has high strength and low weight properties [21]. Then, the printed capsule-shaped design is assembled and coated with epoxy for waterproofing and high strength. The sensing device operates independently with its power system, including a 3.7 V battery and an Arduino Nano microcontroller unit (MCU). It withstands up to 120 °C and is equipped with pH and temperature sensors for real-time data transmission, ensuring efficient retrieval via a robust multifilament fishing line for reliability and durability in the process.

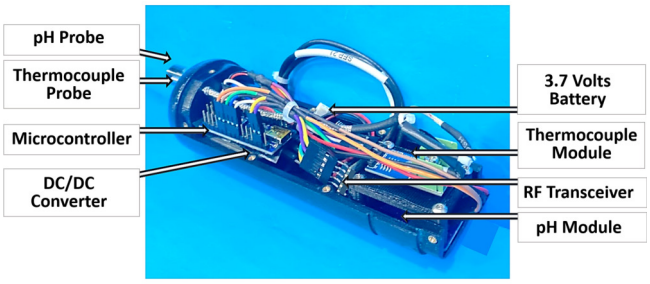

Fig. 22. The capsule-shaped sensing device with pH and temperature sensors and its components for control and communication. The overall weight of the prototype sensing device is 186.9 grams.

Fig. 22 displays the components inside the capsule. A DC/DC converter is used to transform the 3.7 V battery voltage to 5V, providing power to the microcontroller, HC12 wireless serial communication module, pH sensor, and thermocouple module. Positioned externally for precise measurement in crater lake conditions, the waterproof pH probe and thermocouple probe endure temperatures up to 99 °C and 1,260 °C, respectively.

B. Overall System Prototype

The flow chart shown in Fig. 5, presents the various steps to be conducted in order to achieve the objectives of this study. Once the designs are finalized, the fabrication stage begins. A computer-aided design software is utilized to design and model various components, including the sensing device container, component holders, and supporting elements. This ensures precise dimensions and secure placement of the components. To bring the component designs to life, a 3D printer is employed. Careful consideration is given to the selection and design of each component, ensuring they meet the specifications and requirements defined during the design phase. Following the fabrication process, the assembly stage takes place.

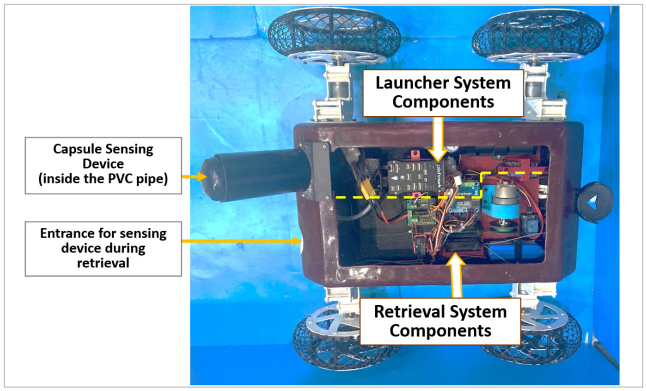

Fig. 23. The inside components of the ground robot for the launcher and retrieval mechanisms, with the retrieval system featuring a supporting mechanism designed to guide the capsule's entry into the ground robot.

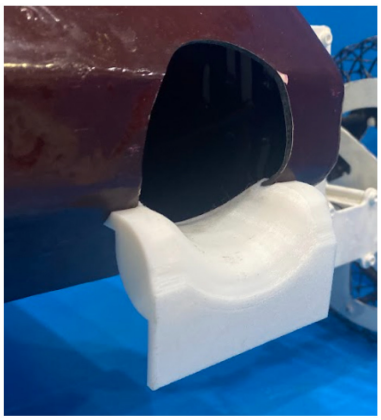

Fig. 24. The capsule supporting mechanism (white-colored component) that is designed to guide the capsule's entry into the robot during the retrieval process.

The individual components are carefully integrated and interconnected, forming a cohesive system. The launcher and retrieval mechanisms are seamlessly integrated into the ground robot as shown in Fig. 23 and 24 showcasing how the system is housed within the ground robot's body. The components of the system are securely held in place utilizing specially designed 3D-printed holders, ensuring stability and proper functioning.

The fabricated sensing device, installed launcher and retrieval systems are installed into the ground robot. The overall assembly and actual prototype is shown in Fig. 25.

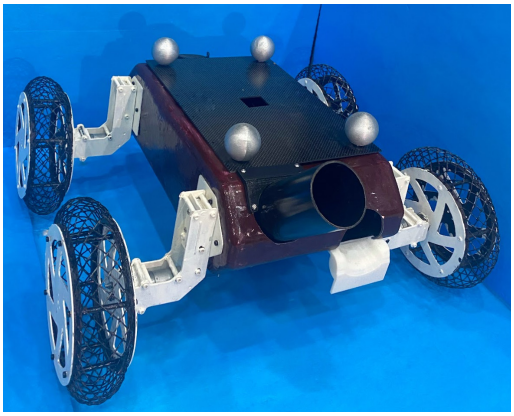

Fig. 25. The actual prototype of the ground robot platform with the installed launcher and retrieval system of the sensing device.

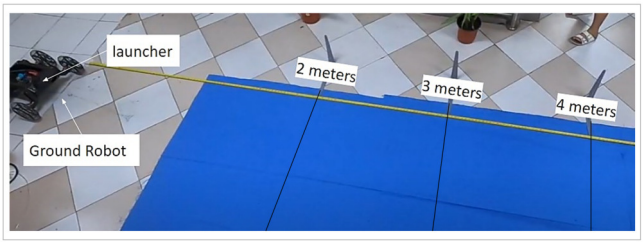

Fig. 26. The test set-up for the sensing device using a dummy capsule tested for a 3-meter launch distance requirement.

C. Sensing Device Launch Test Evaluation

The setup for the launch test is shown in Fig 26. A dummy capsule with the same weight as the original capsule, 186.9g, is used in this test with 2-meter, 3-meter, and 4-meter distances where indicated.

The launch of the capsule-shaped sensing device was swiftly executed, with the compressed pressure necessary to propel the device effectively released through the servo motor. This process was successfully controlled by the radiolink system. Table 1 summarizes the test results, taking into account the required 3-meter distance for launching in the Taal crater lake, with the ground robot positioned 0.5 meters from its shoreline.

TABLE I
SENSING DEVICE LAUNCHING TEST RESULTS

Pressure (MPa)	Sensing Device Launch Distance (m)	Evaluation
1.03	2.83	Not suitable for Taal crater lake application
1.10	2.75	Not suitable for Taal crater lake application
1.17	3.10	Suitable for Taal crater lake application
1.24	3.20	Suitable for Taal crater lake application

D. Sensing Device's pH Sensor Test Evaluation

The results for the pH meter and sensing device's pH sensor reading for three types of liquids are presented in Fig. 27. The pH meter readings yield an average pH of 4.77 for liquid A (matcha latte), 7.683 for liquid B (tap water), and 12.086 for liquid C (bleach). In comparison, the pH sensor provides average readings of 4.6709, 7.8284, and 12.583 pH for the same liquids. The results indicate that the pH levels of liquid A (matcha latte), liquid B (tap water), and liquid C (bleach) are approximately 4.7205, 7.7557, and 12.3345, respectively.

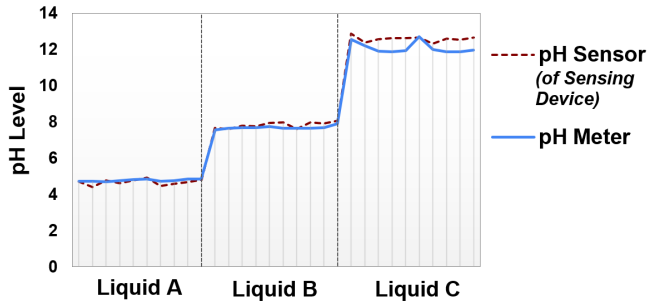

Fig. 27. The test result for pH meter and sensing device's pH sensor reading for three types of liquids: Liquid A (matcha latte), Liquid B (tap water), and Liquid C (bleach).

TABLE II
PH SENSOR AND PH METER COMPARISON

Liquid	pH Sensor	pH Meter	% Difference
1	4.6709	4.77	2.10
2	7.8284	7.683	1.87
3	12.583	12.086	4.03

The average readings obtained from the pH meter and pH sensor show slight variations, with percentage differences ranging from 1.87% to 4.03%. These differences are considered negligible, indicating that both sensors perform satisfactorily and provide reliable pH measurements. The summarized results in Table 2 provide a comprehensive overview of the pH readings obtained from the sensors and highlight the minor deviations between them.

E. Sensing Device's Temperature Sensor Test Evaluation

The acquired set of data, shown in Fig. 28, represents the readings as the sensors are immersed in distilled water, ranging from 80 to 30 degrees Celsius. This process is repeated five times, resulting in 5 data sets (data set A, B, C, D, and E) gathering a total of 60 test data. A linear regression analysis is performed to calibrate the thermocouple, revealing a relationship between the thermocouple readings and the laboratory thermometer values. The equation y = 1.067x - 1.7509 represents this relationship, where y represents the thermocouple reading and x represents the laboratory temperature reading. With the thermocouple calibrated based on this equation, it is tested again.

Table 3 summarizes the calibration results, showing that after calibration, the readings between the thermocouple and the laboratory thermometer exhibit an average difference of 0.44 %. This indicates high accuracy and reliability in the thermocouple's future temperature measurements.

F. Ground Robot with Sensing Device in an Actual Lake Environment

The ground robot with a capsule-shaped sensing device underwent testing in an actual lake environment in Iligan

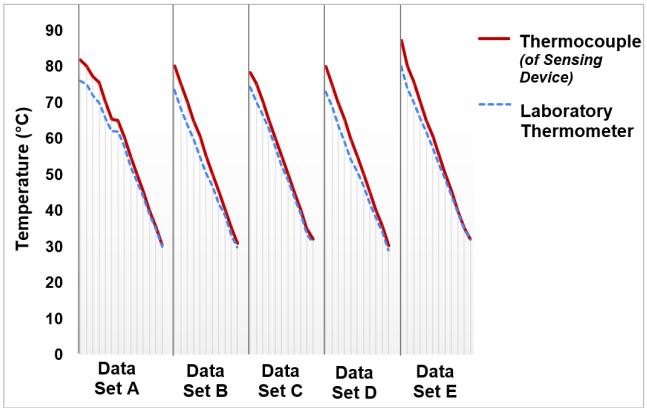

Fig. 28. The test result for laboratory temperature and gas sensing device's thermocouple reading for 60 test data.

TABLE III
TEMPERATURE SENSOR (THERMOCOUPLE) AND LABORATORY THERMOMETER COMPARISON

Test Condition	Temperature Sensor (Thermocouple)	Laboratory Thermometer	% Difference
1	82.01	82	0.012
2	80.14	80	0.175
3	75.07	75	0.093
4	70.00	70	0
5	64.94	65	0.092
6	59.65	60	0.583
7	54.80	55	0.364
8	49.47	50	1.060
9	44.40	45	1.333
10	39.86	40	0.350
11	34.79	35	0.6
12	30.26	30	0.867
13	28.13	28	0.464

City, Philippines. Prior to testing, precautions were taken to ensure the closure of the air valve, absence of air leakage around the valve, and the deactivation of the DC motor. A secure location was carefully chosen to guarantee the robot's safety. To initiate the test, the CO_2 capsule was punctured in its designated holder, and the air pressure was regulated to the desired level. This ensured the controlled release of compressed air to propel the sensing device. Subsequently, the operator remotely controlled the robot to navigate toward the lakeshore, as visually depicted in Fig. 29. Repeated launching-sensing-retrieval of the sensing device were made on other parts of the lake.

Fig. 29. The ground robot remotely controlled to navigate towards the 0.5-meter distance from the lake shore.

The launching process of the sensing device took a 1-second duration. The lake's pH and temperature data were collected in real-time for a 1-minute duration, as required by PHIVOLCS for periodic geochemical data gathering, considering the conditions of the Taal volcano crater lake. Additionally, the lake's pH and temperature were evaluated

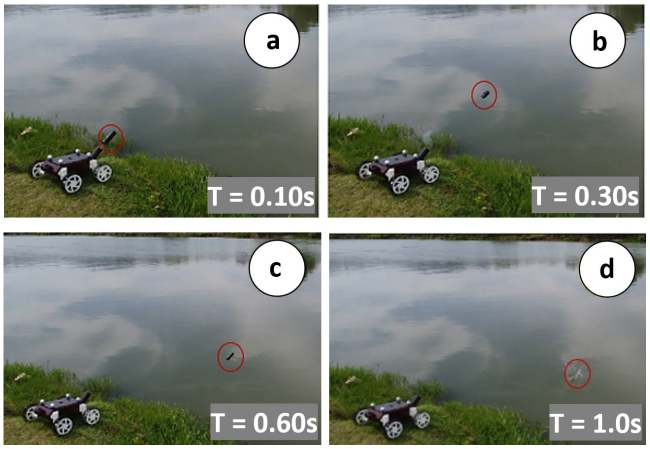

Fig. 30. The launching process of the sensing device in actual lake water. Starting with the initialization of the capsule-launching system (a), and launching at a 3-meter horizontal distance from the ground robot platform (b to e), for a duration of 1-second launching of the sensing device.

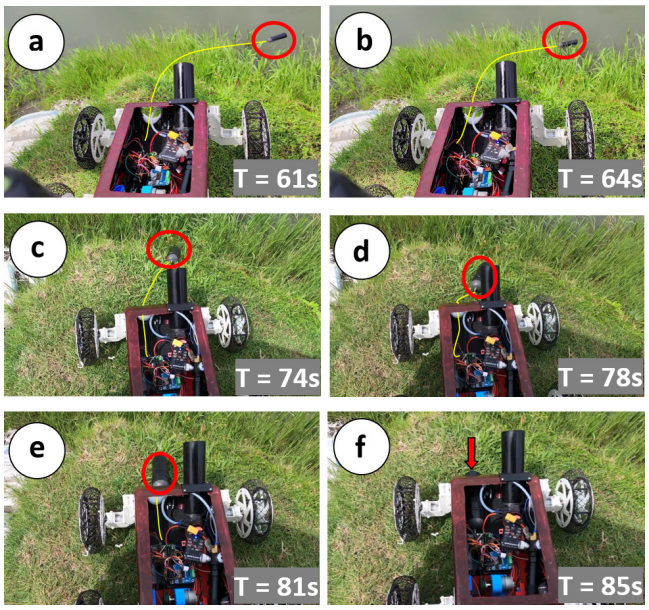

Fig. 31. The retrieval process of the sensing device from the lake water (a-b), after launching the sensing device for 1 second and data gathering for 60 seconds, back to the ground robot platform (c-f) for a duration of 25 seconds of retrieval. The DC motor winds the monofilament line (indicated by the yellow line) connected to the capsule.

using a laboratory pH meter and thermometer with a 1-liter water sample collected from the same area where the capsule was launched, as shown in Fig. 30. The launching process of the sensing device started with the initialization of the capsule-launching system, then launching at a 3-meter horizontal distance from the ground robot platform, which resulted in a duration of 1-second launching of the sensing device.

The retrieval mechanism was thoroughly tested after the launching of the sensing device to assess its reliability and effectiveness. Fig. 31 visually represents the successful retrieval process. The yellow line indicated is the tethered cable of the device connected to the retrieval mechanism component. The system demonstrated its ability to precisely deploy the sensing device into the targeted area and retrieve it securely, all under the operator's command through the remote-control system. The DC motor winds the monofil-

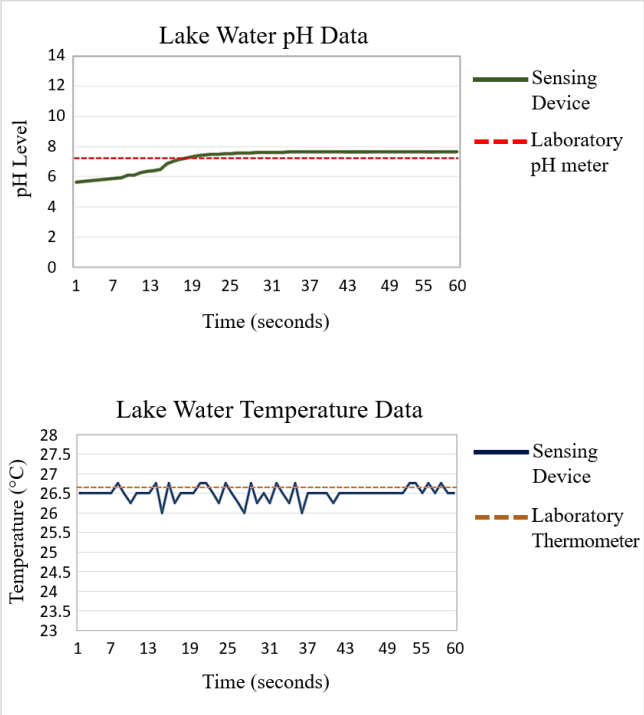

Fig. 32. The gathered real-time pH and temperature data on the actual lake water using the sensing device and its comparison with laboratory devices.

ament line (indicated by the yellow line) connected to the capsule.

To summarize the process, after successfully launching the sensing device for 1 second and data gathering for 60 seconds, the retrieval process took a 25-second duration of successfully retrieving the sensing device into the ground robot.

TABLE IV
SENSING DEVICE'S PH AND TEMPERATURE TEST RESULTS

Sensing Parameter	Sensing Accuracy
pH Sensing	1.8 %
temperature Sensing	0.44 %

Moreover, pH and temperature sensors wirelessly transmitted data using HC12 transceivers and displayed it on the computer's serial monitor. The real-time data gathered for a 1-minute duration was illustrated in Fig. 32. The laboratory pH meter and thermometer were used to verify the test results of the lake's actual pH and temperature data.

As summarized in Table 4, only 1.8% and 0.44% average difference for pH and temperature sensing data error was made by the sensing device, respectively. Thus, the designed sensing device allows accurate real-time data gathering while providing an analysis of the changes in the data gathered with respect to time.

VIII. CONCLUSION

In this study, a sensing device with a launcher and retrieval mechanism was successfully designed for the Taal volcano crater lake application. The launch test demonstrated the system's capability to reach a 3-meter distance from its default position under a pressure of at least 1.17MPa.

Evaluation of the calibrated pH and temperature sensors showed acceptable error levels and negligible differences compared to reference instruments, ensuring reliable data collection. Actual tests in the lake environment further proved the effectiveness of the launching and retrieval system for the sensing device. The integration of remote control, wireless communication, and sensor technology allowed real-time data acquisition from the deployed sensors. Thus, successful data gathering of pH and temperature data from the lake was achieved, resulting in only a 1.8% error for pH reading and a 0.44% error for temperature reading using the sensing device.

Overall, the developed sensing device allows precise real-time data gathering through remote monitoring of temperature and pH data and provides an analysis of the changes in the data gathered over time.

An actual test in a volcano crater lake will further evaluate the developed system in future studies. Several recommendations are proposed to optimize the sensing device's performance based on its robustness. Additionally, expanding the field testing to various terrains and environmental conditions is advised to evaluate the system's versatility and reliability.

REFERENCES

[1] S.-H. You, Y. Gung, C.-H. Lin, K. Konstantinou, T.-M. Chang, E. Chang, and R. Solidum, "A preliminary seismic study of taal volcano, luzon island philippines," *Journal of Asian Earth Sciences*, vol. 65, pp. 100–106, 2013.

[2] R. P. Maximo, A. Bernard, K. Maussen, E. Joiris, and R. Rebadulla, "Geochemical studies of thermal waters from kanlaon volcano, negros island, philippines," *Journal of Volcanology and Geothermal Research*, vol. 374, 2019.

[3] K. Maussen, E. Villacorte, R. R. Rebadulla, R. P. Maximo, V. Debaille, M. A. Bornas, and A. Bernard, "Geochemical characterisation of taal volcano-hydrothermal system and temporal evolution during continued phases of unrest (1991–2017)," *Journal of Volcanology and Geothermal Research*, vol. 352, pp. 38–54, 2018.

[4] J. Zlotnicki, Y. Sasai, J. Toutain, E. Villacorte, M. Harada, P. Yvetot, F. Fauquet, A. Bernard, and T. Nagao, "Electromagnetic and geochemical methods applied to investigations of hydrothermal/volcanic unrests: Examples of taal (philippines) and miyake-jima (japan) volcanoes," *Physics and Chemistry of the Earth, Parts A/B/C*, vol. 34, no. 6, pp. 394–408, 2009.

[5] G. P. J. Varekamp and G. Rowe, "Volcanic lake systematics ii. chemical constraints," *Journal of Volcanology and Geothermal Research*, vol. 97, no. 1, pp. 161–179, 2000.

[6] P. Delmelle, M. Kusakabe, A. Bernard, T. Fischer, S. De Brouwer, and E. Del Mundo, "Geochemical and isotopic evidence for seawater contamination of the hydrothermal system of taal volcano, luzon, the philippines," *Bulletin of volcanology*, vol. 59, pp. 562–576, 1998.

[7] I. M. G. Lariosa, R. M. L. Canlas, J. D. D. Ang, J. C. Pao, C. A. G. Banglos, L. G. Librado, and C. J. O. Salaan, "Drone-based water sampling system with active auto-lock mechanism," in *2022 IEEE 14th International Conference on Humanoid, Nanotechnology, Information Technology, Communication and Control, Environment, and Management (HNICEM)*, pp. 1–6, IEEE, 2022.

[8] P. A. Hernández, G. V. Melián, L. Somoza, M. C. Arpa, N. M. Pérez, E. Bariso, H. Sumino, E. Padrón, J. C. Varekamp, J. Albert-Beltran, *et al.*, "The acid crater lake of taal volcano, philippines: hydrogeochemical and hydroacoustic data related to the 2010–11 volcanic unrest," *Geological Society, London, Special Publications*, vol. 437, no. 1, pp. 131–152, 2017.

[9] G. Muscato, D. Caltabiano, S. Guccione, D. Longo, M. Coltelli, A. Cristaldi, E. Pecora, V. Sacco, P. Sim, *et al.*, "Robovolc: A robot for volcano exploration result of first test campaign," *Industrial Robot: An International Journal*, vol. 30, no. 3, pp. 231–242, 2003.

[10] J. E. Bares and D. S. Wettergreen, "Dante ii: Technical description, results, and lessons learned," *The International Journal of robotics research*, vol. 18, no. 7, pp. 621–649, 1999.

[11] M. Lamboley, C. Proy, L. Rastel, T. N. Trong, A. Zashchirinski, and S. Buslaiev, "Marsokhod: Autonomous navigation tests on a mars-like terrain," *Autonomous Robots*, vol. 2, pp. 345–351, 1995.

[12] Y. Hiroi and A. Ito, "Influence of the height of a robot on comfortableness of verbal interaction," *IAENG International Journal of Computer Science*, vol. 43, no. 4, pp. 447–455, 2016.

[13] N. Uddin, H. Harno, and W. Caesarendra, "Vector-based modeling and trajectory tracking control of autonomous two-wheeled robot," *IAENG International Journal of Computer Science*, vol. 48, no. 4, pp. 1049 – 1055, 2021.

[14] R. L. Cunanan, I. Paradela, C. J. Salaan, and S. Guirnaldo, "Initial development of a mobile robot for aerial-ground collaborative exploration of taal volcano in the philippines," in *2022 IEEE 14th International Conference on Humanoid, Nanotechnology, Information Technology, Communication and Control, Environment, and Management (HNICEM)*, pp. 1–6, IEEE, 2022.

[15] A. Terada, Y. Morita, T. Hashimoto, T. Mori, T. Ohba, M. Yaguchi, and W. Kanda, "Water sampling using a drone at yugama crater lake, kusatsu-shirane volcano, japan," *Earth, Planets and Space*, vol. 70, 2018.

[16] K. Song, A. Brewer, S. Ahmadian, A. Shankar, C. Detweiler, and A. Burgin, "Using unmanned aerial vehicles to sample aquatic ecosystems: Unmanned aerial vehicles in limnology," *Limnology and Oceanography: Methods*, vol. 15, 2017.

[17] A. Flores, D. Scipion, C. Saito, J. Apaza, and M. Milla, "Unmanned aircraft system for andean volcano monitoring and surveillance," in *2019 IEEE International Symposium on Safety, Security, and Rescue Robotics (SSRR)*, pp. 297–302, IEEE, 2019.

[18] S. C. U. Dominguez, J. A. Bolaybolay, E. R. M. Aleluya, and C. J. O. Salaan, "Ground rover visual servo control for drone alignment," in *2022 IEEE 14th International Conference on Humanoid, Nanotechnology, Information Technology, Communication and Control, Environment, and Management (HNICEM)*, pp. 1–6, IEEE, 2022.

[19] K. M. R.C. Juvinall, *Fundamentals of machine component design*. John Wiley Sons, 2019.

[20] J. C. Pao, C. A. G. Banglos, C. J. O. Salaan, and S. A. Guirnaldo, "Simulation and strength analysis of flippable mobile ground robot for volcano exploration and monitoring application," in *2022 IEEE 14th International Conference on Humanoid, Nanotechnology, Information Technology, Communication and Control, Environment, and Management (HNICEM)*, pp. 1–6, IEEE, 2022.

[21] I. Paradela, J. Pao, C. A. Banglos, C. J. Salaan, Y. Ambe, and M. Konyo, "Development of a segmented body serpent robot with active head floating control," *Engineering Letters*, vol. 31, no. 4, pp. 1928–1943, 2023.